Validation of SeaWiFS and MODIS Aqua/Terra aerosol products in coastal regions of European marginal seas

doi:10.5697/oc.55-1.027
OCEANOLOGIA, 55 (1), 2013.
pp. 27–51.

KEYWORDS
Aerosols
Ocean colour
AERONET
Validation
European seas

Frédéric Mélin[1]
Giuseppe Zibordi[1]
Thomas Carlund[2]
Brent N. Holben[3]
Sabina Stefan[4]

[1] European Commission – Joint Research Centre,
Institute for Environment and Sustainability,
TP272, Ispra, 21027, Italy

[2] Swedish Meteorological and Hydrological Institute,
SE-601 76, Norrköping, Sweden

[3] Goddard Space Flight Center,
National Aeronautics and Space Administration,
Greenbelt, Maryland 20771, USA

[4] University of Bucharest,
Faculty of Physics,
077125 Magurele, P.O. BOX MG-11, Bucharest, Romania

Received 5 September 2012, revised 26 November 2012, accepted 18 December 2012.

Abstract

The aerosol products associated with the ocean colour missions SeaWiFS and MODIS (both Aqua and Terra) are assessed with AERONET field measurements collected in four European marginal seas for which fairly large uncertainties in ocean colour in-water products have been documented: the northern Adriatic, the

Baltic, Black and North Seas. On average, more than 500 match-ups are found for each basin and satellite mission, showing an overall consistency of validation statistics across the three missions. The median absolute relative difference between satellite and field values of aerosol optical thickness τ_a at 443 nm varies from 12% to 15% for the three missions at the northern Adriatic and Black Sea sites, and from 13% to 26% for the Baltic and North Sea sites. It is in the interval 16–31% for the near-infrared band. The spectral shape of τ_a is well reproduced with a median bias of the Ångström exponent varying between −15% and +14%, which represents a clear improvement with respect to previous versions of the atmospheric correction scheme. These results show that the uncertainty associated with τ_a in the considered coastal waters of the European marginal seas is comparable to global validation statistics.

1. Introduction

Ocean colour products have become an important asset for understanding the dynamics of coastal/shelf regions and marginal seas by providing information on the distributions of quantities such as the concentration of chlorophyll *a*, suspended particles or chromophoric dissolved organic matter. On the other hand, relatively large uncertainties affect such ocean colour products in optically complex waters, including the European seas and coastal areas (e.g. Blondeau-Patissier et al. 2004, Darecki & Stramski 2004, Lavender et al. 2004, Sancak et al. 2005, Mélin et al. 2007a). The sources of error are associated with the bio-optical algorithms used to quantify the optically significant constituents in the water, and with the input to these algorithms, i.e. the spectrum of remote sensing reflectance, R_{RS}. In turn the uncertainties associated with R_{RS} found in coastal areas and marginal seas (e.g. Zibordi et al. 2009, 2011) can be explained by different factors that are inherent to these regions. These include the presence of aerosols with a higher concentration and more complex optical properties (particularly higher levels of absorption) with respect to the open ocean.

The objective of this paper is to assess the uncertainties found in the determination of aerosols in European coastal regions by the atmospheric correction schemes specific to the ocean colour missions Sea-viewing Wide Field-of-View Sensor (SeaWiFS, McClain et al. 1998) and Moderate Resolution Spectroradiometer (MODIS on board Aqua and Terra, Esaias et al. 1998). The focus is on European regions with rather turbid waters and for which fairly large uncertainties in in-water products derived from ocean colour have been documented, namely, the northern Adriatic and the Baltic, Black and North Seas. The approach relies on the availability

of an abundant record of field data collected at measurement sites of the Aerosol Robotic Network (AERONET, Holben et al. 1998) located in the regions considered. The uncertainties associated with the remote sensing products are estimated by comparison with field observations of aerosol optical thickness and Ångström exponent, under the basic assumption that uncertainties associated with the latter are small compared to those affecting the satellite products. First, field and satellite data are introduced and the method of analysis is described. The validation results are then presented for each region and discussed.

2. Material and methods

2.1. AERONET Data

AERONET stations are equipped with automated sun-photometers (CIMEL, France) that measure the direct solar irradiance used to derive the aerosol optical thickness τ_a at various wavelengths λ. All the data used in the present work are so-called Level-2, i.e. obtained after cloud-screening and full quality control (Holben et al. 1998, Smirnov et al. 2000, 2004). Values of τ_a at the centre-wavelengths close to 440, 500, 670 and 870 nm are considered for the analysis, when available. The Ångström exponent α is derived by linear regression of log-transformed τ_a as a function of wavelength λ in the interval 440–870 nm. The expected uncertainty for τ_a for visible and NIR wavelengths is 0.010–0.015 (Eck et al. 1999, Schmid et al. 1999). Uncertainties associated with the automated cloud-screening procedures could introduce additional uncertainty for some data records (McArthur et al. 2003).

The AERONET data used in this work were collected at 10 sites associated with 4 European marginal seas (Table 1, Figure 1): i) the Adriatic Sea, represented by the Venice site, actually the Aqua Alta Oceanographic Tower (AAOT) off the Venice lagoon; ii) the Baltic Sea with two sites located on light towers, along the Swedish coast (Gustav Dalén Light Tower, GDLT) and in the Gulf of Finland (Helsinki Lighthouse Tower, HLT), and one site located on Gotland island; iii) the North Sea with four stations distributed along the coast, from Dunkerque (DUNK), Oostende (OOST), The Hague (THAG) to the island of Helgoland (HELG); iv) the Black Sea with the sites of Eforie (EFOR) on the north-west coast and Sevastopol (SEVA) on the Crimean peninsula. All the sites are located very near the coast and lie at altitudes from 0 to 80 m (average 26 m).

The deployment period varies between stations and is not always continuous (for instance, high latitude sites are often not operated in

Table 1. List of sites used in the analysis. The first column gives the name of the site as defined in the AERONET data base, and the second column gives the corresponding acronym used in the present work on the figures. Several sites are grouped for the three basins – the Baltic, North and Black Seas. The third to fifth columns list the number of match-ups found for SeaWiFS, MODIS Aqua and Terra for each basin or site. The sixth and seventh columns display the median values derived from AERONET observations over the match-up sets for each basin or site. The values are given as intervals defined by the three sensors

Region/Site	Acronym	SWF	MOD-A	MOD-T	$\tau_a(443)$	α
Venice	AAOT	942	861	898	0.20–0.24	1.60–1.65
Baltic Sea	BALT	319	675	746	0.11–0.13	1.46–1.49
Gotland	GOTL	174	74	139	0.12–0.13	1.37–1.49
Gustav_Dalén_Tower	GDLT	62	302	315	0.10–0.13	1.46–1.64
Helsinki_Lighthouse	HLT	83	299	292	0.10–0.12	1.49–1.55
North Sea	NORS	358	587	637	0.17–0.21	1.40–1.46
Dunkerque	DUNK	75	178	198	0.16–0.22	1.32–1.40
Helgoland	HELG	108	205	215	0.17–0.18	1.31–1.53
Oostende	OOST	124	153	141	0.18–0.23	1.47–160
The Hague	THAG	51	51	83	0.19–0.20	1.29–1.54
Black Sea	BLCK	182	536	599	0.19–0.23	1.51–1.55
Eforie	EFOR	30	105	101	0.21–0.24	1.43–1.60
Sevastopol	SEVA	152	431	498	0.19–0.22	1.50–1.56

winter). The longest record is that of AAOT, starting in June 1999 (as Level-2 data), and four sites have close to ten years of operation (AAOT, Dunkerque, Helgoland and Oostende), while for two sites the time series is currently terminated (1999–2004 for Gotland, 2001–2006 for The Hague). The two Black Sea stations and the two towers in the Baltic Sea started operating between 2005 and 2009.

2.2. Satellite data

The satellite imagery is processed with the SeaWiFS Data Analysis System (SeaDAS, version 6, Fu et al. 1998) applied to SeaWiFS, MODIS-A (on-board Aqua) and MODIS-T (on-board Terra) Level-1A top-of-atmosphere (TOA) data. For SeaWiFS, only full-resolution (Local Area Coverage, LAC) images are considered. The satellite data have been processed with the latest calibration tables, which should minimize the

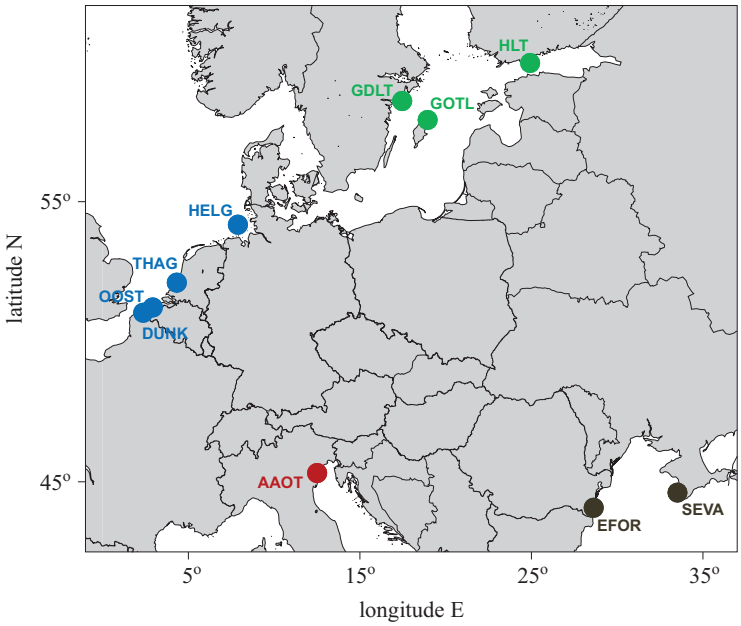

Figure 1. Location of the AERONET validation sites. The acronyms are defined in Table 1

degradation of satellite products resulting from uncorrected sensor drift (Zibordi et al. 2012). Furthermore, only aerosol satellite products associated with ocean colour data processing are analysed in this work.

The atmospheric correction follows the principles found in Gordon & Wang (1994) with subsequent evolutions (see Franz et al. 2007, and references therein). Further updates include a modified bio-optical modelling in the near-infrared (NIR, Bailey et al. 2010) and a change of the aerosol models considered candidates to represent the aerosol component in the atmospheric correction process (Ahmad et al. 2010). This latter update replaced the twelve original aerosol models (Shettle & Fenn 1979, Gordon & Wang 1994) with a set of 80 models that depend on atmospheric relative humidity (RH, 8 values) and the fraction of fine particles in the aerosol size distribution (f, 10 values).

The process of atmospheric correction can be summarized as follows. The ratio of the aerosol reflectance ρ_a at the 2 NIR bands is first computed assuming a negligible contribution from the water-leaving reflectance. By varying f the two aerosol models with the associated ρ_a ratio closest to (i.e. just above and below) the observed one are selected. This search is conducted with the two families of aerosol models with RH values closest to the observed RH as given by meteorological 6-hourly data from the National

Centers for Environmental Prediction (NCEP). The aerosol contribution is then a weighted average of the contribution from the four selected models. A possible contribution from the water-leaving reflectance in the NIR is handled through an iterative process. SeaDAS only allows saving in its Level-2 outputs the aerosol model numbers associated with the RH closest to the observed value, so that statistics on the selected aerosol model numbers are only approximations.

All the satellite imagery associated with the selected measurement sites (Figure 1) is processed and extracts of 31×31 pixels centred on the site location are saved with the following information: the remote sensing reflectance R_{RS} and aerosol optical thickness τ_a spectra, the numbers of the two aerosol models selected for atmospheric correction and their relative contribution to the aerosol reflectance, viewing and illumination geometry and ancillary information. SeaWiFS spectral values are provided at wavelengths 412, 443, 490, 510, 555, 670, 765 and 865 nm, while the band set for the MODIS sensors includes 412, 443, 488, 531, 547, 667, 748 and 869 nm. The Ångström exponent is computed by linear interpolation of the log-transformed τ_a as a function of wavelength λ in the interval 443 nm to the longest NIR bands, omitting 765 nm or 748 nm for SeaWiFS and MODIS, respectively, for consistency with the wavelengths characterizing the field measurements.

Additionally, the full SeaWiFS LAC archive has been processed for the European seas for the period 1997–2004 to derive monthly maps of ocean colour products. In this work, multi-annual averages of $\tau_a(443)$ and α are used for illustration.

2.3. Match-up selection

The match-up selection protocol has been fully described by Mélin et al. (2010) and is briefly summarized here. A potential match-up is defined as the association of a satellite extract with the field observations available in a ± 1 h time window centred on the overpass time. In the extract, the pixels considered for analysis are those not affected by the standard processing flags (Bailey & Werdell 2006) excluding cases of atmospheric correction failure, the presence of stray light, the detection of land, cloud or ice, excessive satellite or solar zenith angles. Pixels with negative R_{RS} between 412 nm and the green band (555 and 547 nm for SeaWiFS and MODIS, respectively) are also excluded. The closest 5×5-pixel square with all valid retrievals is searched and possibly expanded in larger rectangles if all pixels are still associated with valid values. The satellite value to be compared

with field observations is the average over the available pixels. This match-up selection protocol is constrained by the fact that most validation sites are actually located on land, which implies that the satellite pixels do not exactly match the measurement location. An underlying assumption is that the satellite value, computed for a significant number of adjacent pixels fairly close to the site, is representative of the area and can be compared with the field value. It is also assumed that the satellite retrieval is not overly perturbed by the presence of a land mass and/or shallow waters. It can thus be argued that the differences between the satellite and field values documented here could be higher than those that would be found in ideal validation conditions. The issue of spatial mismatch was addressed in detail by Mélin et al. (2010), who showed that variations in the match-up selection protocol do not affect the results significantly.

The satellite value is compared with the average of AERONET data in the time interval of ± 1 hour around the satellite overpass. To ensure representative conditions, these data are considered only if at least three field observations were performed in this time interval with a coefficient of variation (CV, ratio of standard deviation and average) $< 20\%$ for $\tau_{\mathrm{a}}(870)$. Similarly, satellite values are excluded if the CV (computed over the considered pixels) is $> 20\%$ for τ_{a} in the NIR in order to avoid spatially heterogeneous conditions.

To compare field and satellite values at slightly different wavelengths, band shift corrections are applied. For neighbouring wavelengths (e.g. 443 and 440 nm, 865 and 870 nm), the field value is expressed at the satellite wavelength through a 2nd-order polynomial fit to the logarithm of τ_{a} as a function of λ (O'Neill et al. 2001, Mélin et al. 2007b). The same approach is applied to derive a synthetic satellite value at 500 nm for comparison with AERONET data (this band is present in most AERONET series). The error associated with this calculation is minimal since the satellite τ_{a} are linear combinations of modelled spectra that are well represented by a 2nd-order polynomial fit.

Considering N match-ups, the differences between AERONET (AER) and satellite (SAT) values of the quantity x are expressed through the median of absolute relative differences ($|\psi|$, in %), relative differences (ψ, in %), absolute differences ($|\delta|$) and differences (δ):

$$|\psi| = 100 \times median \left(\frac{|x_i^{\mathrm{SAT}} - x_i^{\mathrm{AER}}|}{x_i^{\mathrm{AER}}} \right)_{i=1,\,N}, \tag{1}$$

$$\psi = 100 \times median \left(\frac{x_i^{\mathrm{SAT}} - x_i^{\mathrm{AER}}}{x_i^{\mathrm{AER}}} \right)_{i=1,\,N}, \tag{2}$$

$$|\delta| = median\left(|x_i^{\mathrm{SAT}} - x_i^{\mathrm{AER}}|\right)_{i=1,\,N}\ , \tag{3}$$

$$\delta = median\left(x_i^{\mathrm{SAT}} - x_i^{\mathrm{AER}}\right)_{i=1,\,N}\ . \tag{4}$$

The values of $|\delta|$ and δ represent the uncertainty and bias associated with x^{SAT} in units of x, assuming x^{AER} is exact. The use of the median operator is preferred so as to lessen the impact of outliers on statistics.

3. Results

The seasonal distributions of match-ups are illustrated in Figure 2 for each basin. For all four regions, there is a clear annual cycle in the number of match-ups with maxima from June to August and minima (or no match-ups) in winter. This is consistent with meteorological conditions (like cloud cover) that prevent ocean colour and/or AERONET observations

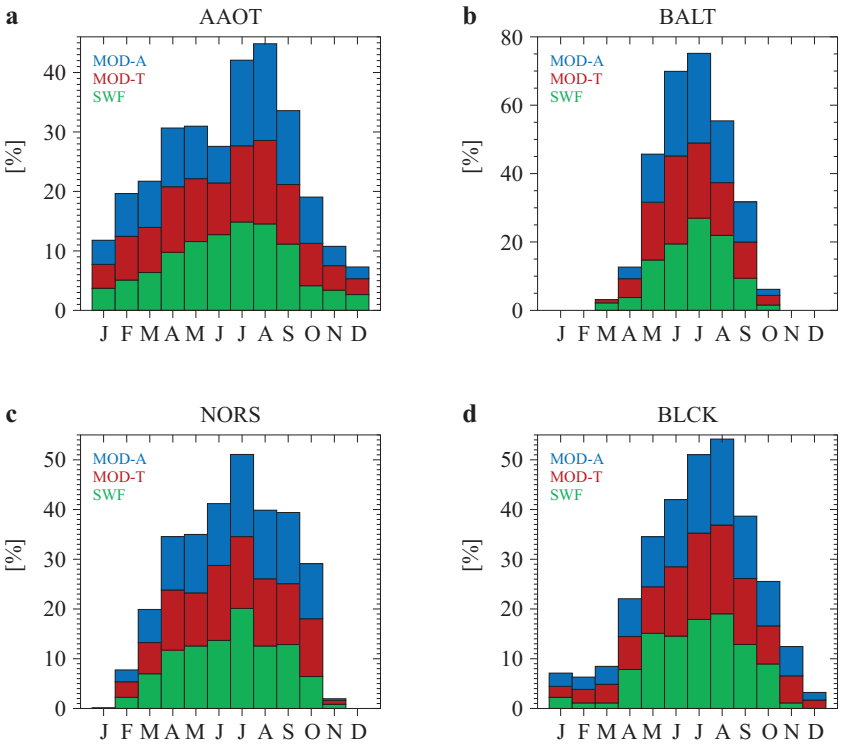

Figure 2. Average monthly distribution of the number of match-ups during the year for the 4 regions: a) AAOT, b) Baltic Sea, c) North Sea and d) Black Sea

more frequently in winter. In that season, the solar zenith angle at high latitudes may also exceed the maximum allowed for ocean colour processing (70°). Finally, some AERONET deployments are suspended during winter (e.g. GDLT and HLT). The number of match-ups for each sensor and basin exceeds 350 (except 182 for SeaWiFS in the Black Sea), with the number of match-ups per site going from 30 (for SeaWiFS at the Eforie site) to 942 (SeaWiFS at AAOT). These numbers may be lower at 500 nm depending on the spectral configuration of the field instrument operated at the various sites. In the following sections, the red band means 670 nm for SeaWiFS or 667 nm for MODIS, and the NIR band refers to 865 nm for SeaWiFS and 869 nm for MODIS. Validation results are now presented for each basin in the following sections and in Figures 4 to 7, while Table 2 provides a summary of the results for the four basins. To provide a regional perspective with respect to the single sites, Figure 3 shows multi-annual averages of SeaWiFS-derived $\tau_a(443)$ and α for the Adriatic, Baltic, North and Black Seas.

3.1. Northern Adriatic Sea

The median values of the AERONET α for the AAOT site lie within the interval 1.60–1.65 for the three match-up sets (Table 1), which is fairly representative of the values observed at this site, strongly influenced as it is by anthropogenic aerosols from the Po Valley (Mélin & Zibordi 2005, Mélin et al. 2006, Clerici & Mélin 2008). Similar values are also found for the rest of the Adriatic basin, even though the average α tends to decrease southwards (Figure 3b). The validation results for $\tau_a(443)$ exhibit $|\psi|$ values varying from 12% to 14% (Figure 4). Generally, the value of $|\psi|$ tends to increase spectrally: for SeaWiFS, it is 13–14% from 443 to 670 nm, and 16% at 865 nm, while for both MODIS sensors, it is in the interval 16–20% for wavelengths 667 and 869 nm. This increase can be partly explained by the relatively higher noise that characterizes the lower τ_a signals usually observed at longer wavelengths. In the case of MODIS-T, the increase in $|\psi|$ is associated with an increase in the bias ψ, from +3% to +15% from 443 to 869 nm. This spectral variation of ψ is consistent with the negative bias seen for α of −13% (Figure 4f, δ equal to −0.20). This being said, the magnitudes of ψ are mostly below 10%, and the distributions of α are fairly unbiased (ψ of −3% and −1%, or δ of −0.05 and −0.01, for SeaWiFS and MODIS-A respectively). Satellite τ_a are generally too high for low values while they underestimate high τ_a values (Figure 4a–c for 443 nm).

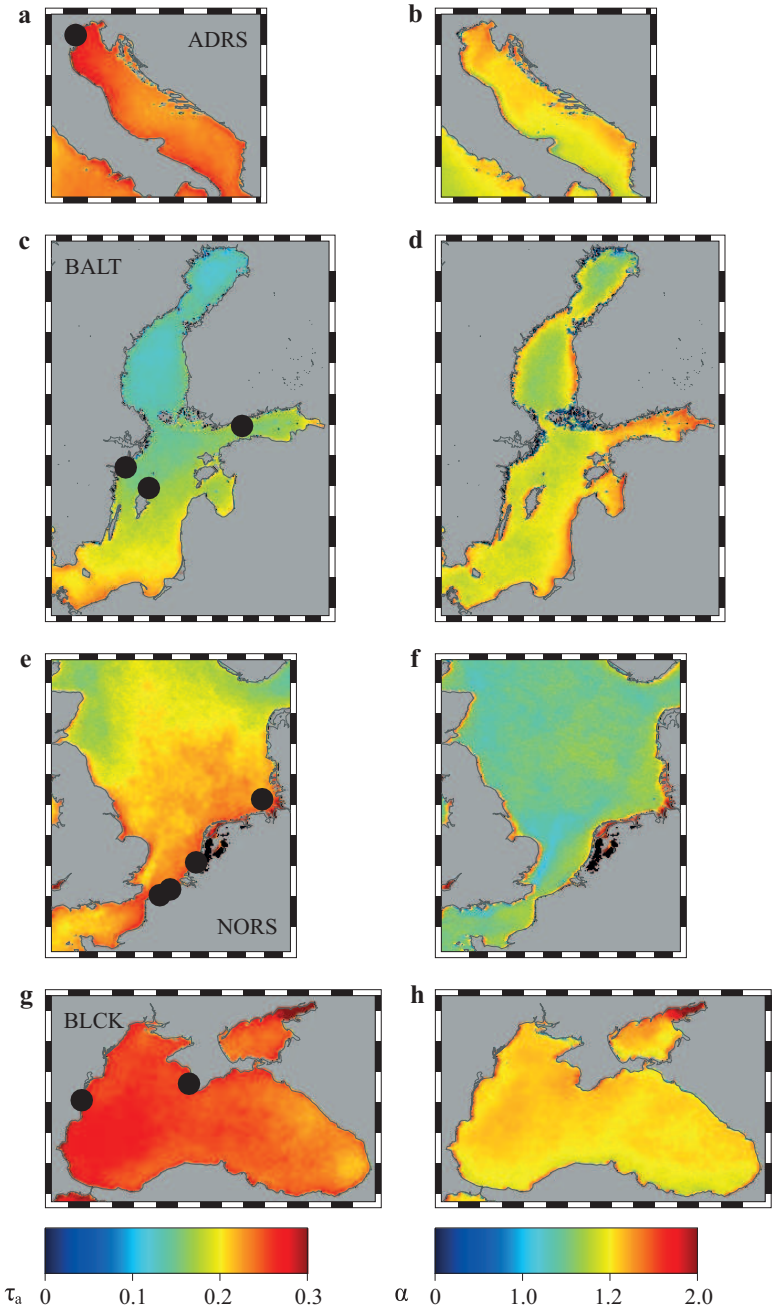

Figure 3. SeaWiFS-derived climatological annual average (1997–2004) for τ_a at 443 nm (left-hand column) and α (right-hand column) for the Adriatic Sea (a, b), the Baltic Sea (c, d), the North Sea (e, f) and the Black Sea (g, h). The black filled circles show the positions of the validation sites in each basin (see Figure 1)

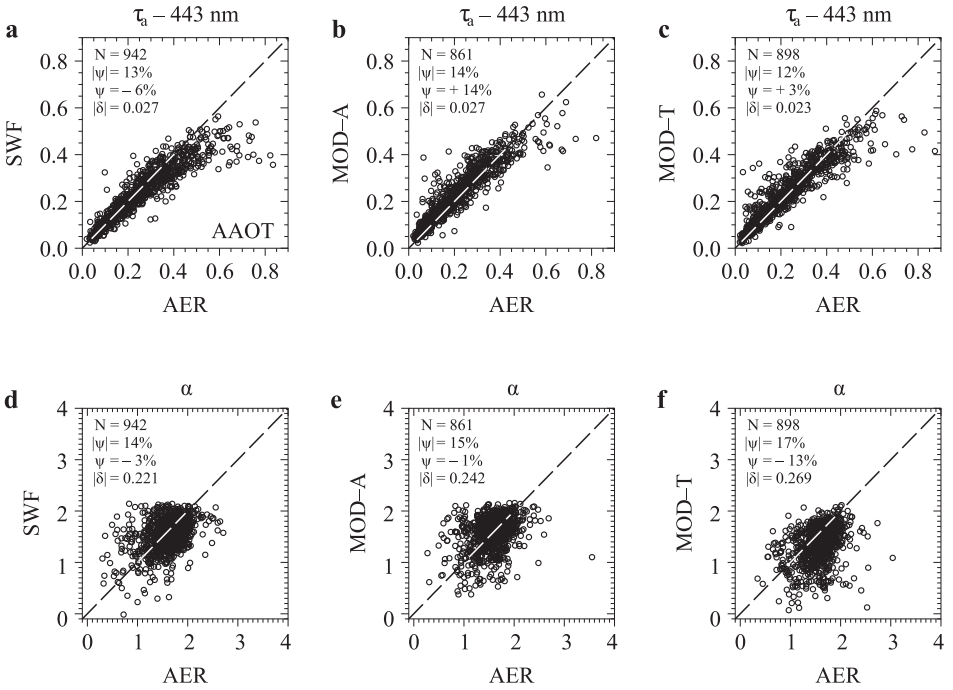

Figure 4. Scatterplot for the AAOT site for τ_a at 443 nm (a, b, c) and α (d, e, f), for SeaWiFS (a, d), MODIS-Aqua (b, e) and MODIS-Terra (c, f). The statistics are defined in the text

3.2. Baltic Sea

With respect to the statistics found at other sites, the AERONET median values associated with the Baltic match-up sets are lower for α (1.46–1.49) and much lower for $\tau_a(443)$ (by a factor of 2, Table 1), which means that the aerosol load is likely to be limited by a smaller number of aerosol sources, westerly winds transport and precipitation scavenging. The lower τ_a compared to the other regions are confirmed by synoptic satellite products from the MODIS atmosphere project (Koelemeijer et al. 2006) and by Figure 3c, which also illustrates an increasing north-south gradient of τ_a. Even though the median α still suggests continental and anthropogenic influences, the lower values indicate a relatively greater maritime input with respect to the other sites. In this closed basin, the aerosol variability and the relative weight of different sources are highly dependent on the wind direction (Zdun et al. 2011). The distribution of α associated with the match-ups is fairly typical of values found at other sites around the central/northern Baltic Sea for the summer season (Toledano et al. 2012). Figure 3d also shows spatial variations of α, with slightly lower values

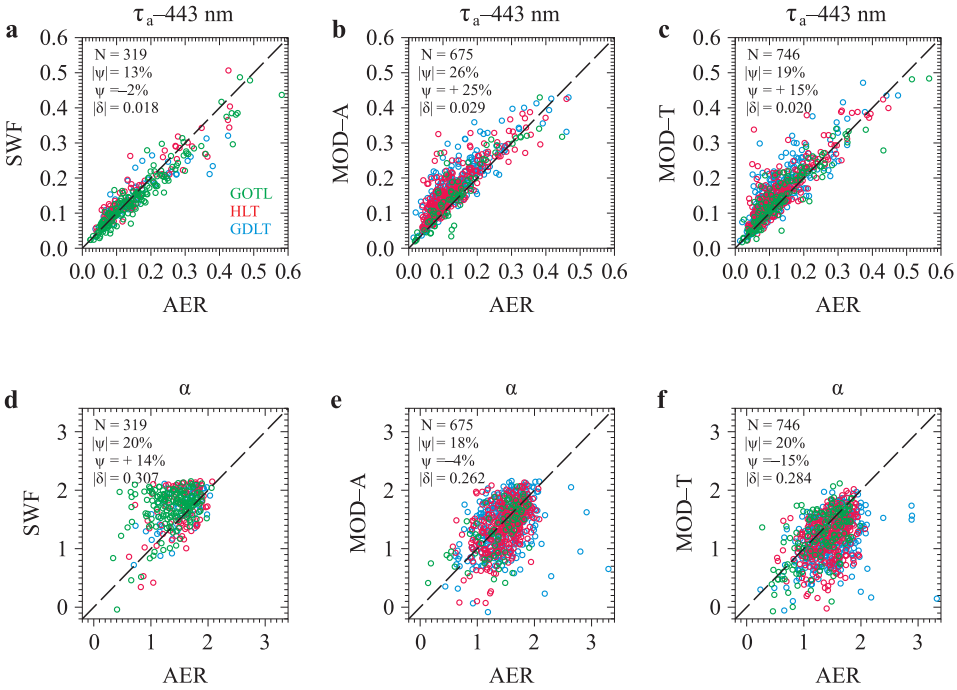

Figure 5. As for Figure 3 for the Baltic Sea sites. Match-ups in green, brown-red and blue are for Gotland, the Helsinki Lighthouse Tower and the Gustav Dalén Light Tower respectively

in the Gulf of Bothnia and higher values in the Gulfs of Riga and Finland.

The validation results are fairly similar to those found at AAOT for SeaWiFS, with $|\psi|$ increasing from 13% at 443 nm to 21% at 865 nm, and showing slightly negative biases (Figure 5a). The differences are greater for both MODIS, with $|\psi|$ above 18% at all wavelengths, again as a result of higher biases ψ that have a maximum at 667 nm (+39% and +34% for MODIS-A and MODIS-T respectively). This degraded uncertainty at 667 nm could have an impact on the atmospheric correction and results of R_{RS} at a wavelength for which the R_{RS} signal found in the Baltic Sea is relatively high (Zibordi et al. 2009). Even though the relative differences $|\psi|$ are higher than at AAOT, the median absolute differences $|\delta|$ are comparable (0.010 to 0.029, Table 2). The spectral shape of τ_a is well represented (Figure 5d–f), with a slight overestimate of α for SeaWiFS (+14%), a bias close to null for MODIS-A (−4%) and a slight underestimate for MODIS-T (−15%), while $|\psi|$ is approximately 20%.

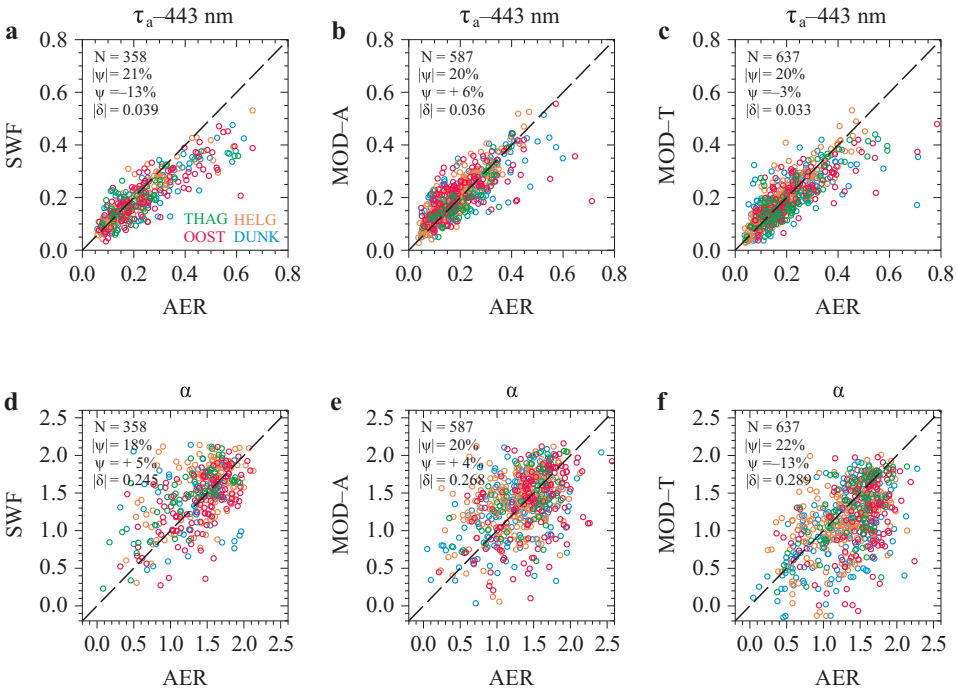

Figure 6. As for Figure 3 for the North Sea sites. Match-ups in green, brown-red, orange and blue are for The Hague, Oostende, Helgoland and Dunkerque respectively

3.3. North Sea

Median AERONET statistics for α are similar to those of the Baltic sites (1.40–1.46), with some variations between sites. This does not apply to the open North Sea, where the average α is lower (Figure 3f). The Dunkerque site has the smallest median α. The aerosols are a mixture dependent on the air mass trajectories from the Atlantic sector and from land (Ebert et al. 2000, Kuśmierczyk-Michulec et al. 2007), with the values of α pointing to the importance of continental inputs. The validation results are very close for all three missions, with $|\psi|$ of 19–21% at all wavelengths (except 23% at 865 nm for SeaWiFS, and 25% at 869 nm for MODIS-T). These differences are associated with significant biases for SeaWiFS (−12% to −18%) but this is less so for both MODIS (ψ less than 10% in magnitude). As at AAOT, high τ_a are underestimated by SeaWiFS (Figure 6a). The median absolute differences $|\delta|$ are the highest of the four groups of sites, above 0.033 at 443 nm (Table 2). Even though the match-up distribution for α is fairly scattered ($|\psi|$ of the order of 20%, $|\delta|$ from 0.24 to 0.29, Figure 5d–f), it is well on the 1:1 line with ψ between −13% (MODIS-T) and +5% (SeaWiFS).

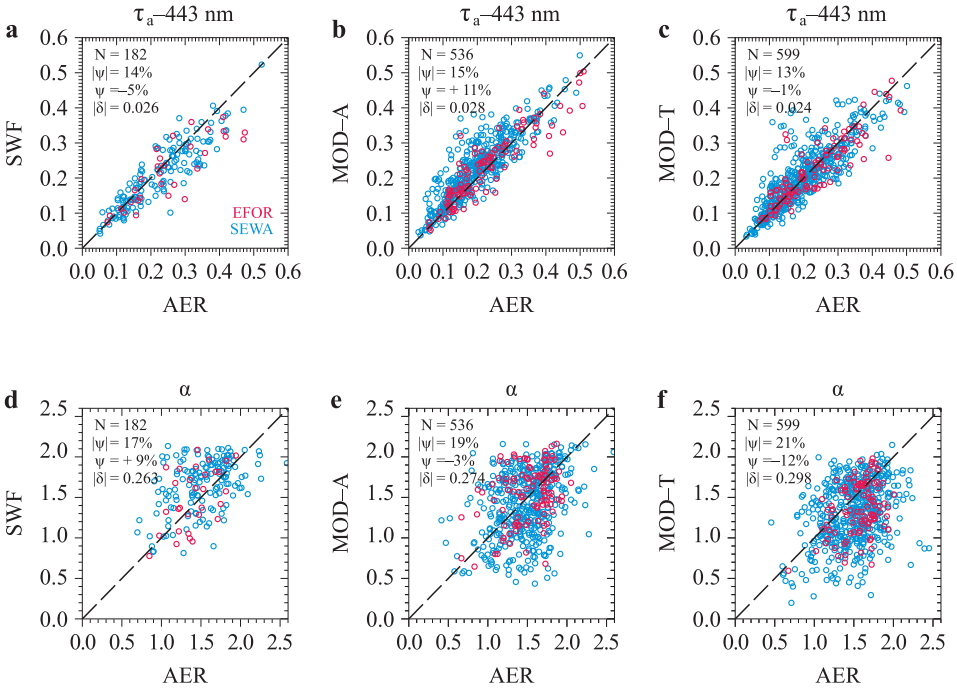

Figure 7. As for Figure 3 for the Black Sea sites. Match-ups in brown-red and blue are for Eforie and Sevastopol respectively

3.4. Black Sea

The median values of α observed for the Black Sea are 1.51–1.55, between the values found in the northern seas and the northern Adriatic, while the magnitude of τ_a is similar to that of the North Sea and Adriatic sites (Table 1). At basin level, the Black Sea shows the highest average τ_a (Figure 3g). The values of α again indicate the strong influence of continental aerosols, associated with the relatively large sulphate loads found in south-eastern Europe (Marmer et al. 2007), and seasonally including inputs from agricultural waste burning (Sciare et al. 2008).

For SeaWiFS, $|\psi|$ varies from 14% at 443 nm to 17% at 670 nm, and reaches 24% at 865 nm, an increase associated with a larger bias (−15%, Table 2). In turn, this is translated by a positive bias for α (+9%, Figure 7d). The results in terms of $|\psi|$ for both MODIS are almost identical to those of SeaWiFS, but are associated with slightly positive biases across the spectrum (+10% to +14% for MODIS-A, −1% to +10% for MODIS-T). The Ångström exponent is slightly underestimated for MODIS (−3% for MODIS-A, −12% for MODIS-T). All $|\delta|$ values for τ_a are in the interval 0.015 to 0.026.

Table 2. Validation statistics in the four regions (by column) for τ_a derived from SeaWiFS (SWF), MODIS-A and MODIS-T, expressed as $|\psi|$ (in %), ψ (in %) and $|\delta|$ (in the unit of τ_a)

Region	AAOT	BALT	NORS	BLCK
SWF	$\tau_a(443)$			
$\|\psi\|$[%]	13	13	21	14
ψ[%]	−6	−2	−13	−5
$\|\delta\|$	0.027	0.018	0.039	0.026
	$\tau_a(865)$			
$\|\psi\|$[%]	16	21	23	24
ψ[%]	−4	−15	−18	−15
$\|\delta\|$	0.012	0.010	0.018	0.017
MOD-A	$\tau_a(443)$			
$\|\psi\|$[%]	14	26	20	15
ψ[%]	+9	+25	+6	+10
$\|\delta\|$	0.027	0.029	0.036	0.028
	$\tau_a(869)$			
$\|\psi\|$[%]	18	28	22	23
ψ[%]	+5	+27	+4	+11
$\|\delta\|$	0.012	0.012	0.016	0.016
MOD-T	$\tau_a(443)$			
$\|\psi\|$[%]	12	19	20	13
ψ[%]	+3	+15	−3	−1
$\|\delta\|$	0.023	0.020	0.033	0.024
	$\tau_a(869)$			
$\|\psi\|$[%]	20	31	25	21
ψ[%]	+15	+29	+9	+10
$\|\delta\|$	0.015	0.013	0.018	0.015

4. Discussion

4.1. Aerosol models

For all four basins and three missions, the bias δ obtained for the Ångström exponent is in the interval from −0.216 to +0.213 in units of α (or from −15% to +14% in relative terms). Even though there is still

a significant dispersion of match-up points, the distributions of α are found around the 1:1 line. This represents a clear improvement with respect to previous versions of the atmospheric correction scheme (i.e. SeaDAS version 5 or less): a bias of -0.52 was found for α from a global match-up set for SeaWiFS and MODIS-A that increased to -0.70 and -0.59 for SeaWiFS and MODIS-A respectively, when AERONET European continental sites were considered (Mélin et al. 2010). This was associated with an increasing bias for τ_{a} from 443 nm to the NIR bands, for which biases above 50% were typical. Carlund et al. (2005) also documented a large underestimate of α for SeaWiFS for the site of Gotland.

This improvement in the representation of the spectral shape of τ_{a} results from several changes in the atmospheric correction, particularly a revised bio-optical modelling in the NIR (Bailey et al. 2010) and updated aerosol models (Ahmad et al. 2010). The former element has an effect on the choice of aerosol model that is based on the ratios of aerosol reflectance at the 2 NIR bands, but a dedicated study would be required to separate this effect from the introduction of revised aerosol models. To further document the aerosol models associated with the match-up populations, Figure 8 shows the related frequency distributions of selected models as a function of the fine-mode fraction f for each set of relative humidity (RH). The frequency distributions are computed including all pixels accepted in the match-up selection process.

For the four basins, most of the selected aerosol models are associated with RH of 50% or 70% as imposed by the meteorological conditions provided by NCEP products (the low values of RH are partly the result of the clear sky conditions associated with ocean colour match-ups). Overall, the most frequently selected aerosol model is RH50f50 (i.e. RH of 50% and f of 50%), with relative frequencies above 20% for SeaWiFS and MODIS-A at AAOT and the Black Sea sites. In general 3 to 5 models can explain more than 50% of the frequencies of selection, with f from 20% to 80% and RH of 50% and 70%. As expected from the validation statistics, the histograms are fairly consistent between missions, even though some subtle differences can be noticed. For instance, in the Baltic Sea, the frequency distribution is shifted towards slightly higher α for SeaWiFS, with the most frequently selected models being RH50f50 and RH70f50 (13%). This is consistent with the positive bias found with respect to field data of α (Figure 5d). A more complete assessment of the most frequently selected models, for instance, with additional data such as single scattering albedo and scattering phase function, could lead to a refinement of the models and a further improvement of the atmospheric correction for European coastal waters.

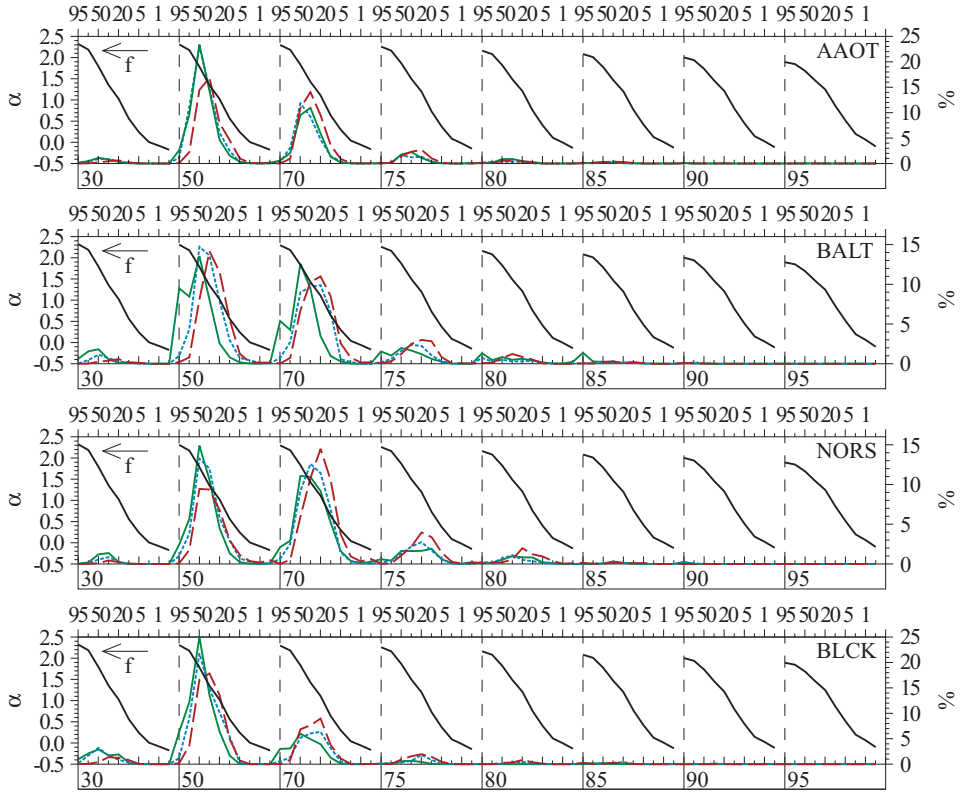

Figure 8. Frequency distribution of selected aerosol models (given as a percentage on the right-hand axis). The green lines denote SeaWiFS, the dotted blue lines MODIS-A and the brown dashed lines MODIS-T. The upper axis shows the fine-mode fraction f repeated for each RH value (separated by the vertical dashed lines, with RH given in the rectangle along the lower axis). The values of f increase from right to left following the arrow (0, 1, 2, 5, 10, 20, 30, 50, 80, 95, in %). The Ångström exponent α for each model is indicated by the black line (with the scale on the left-hand axis)

4.2. Consistency of τ_a uncertainties between missions and sites

Overall, the uncertainties documented in Section 3 show a relative consistency between sites and missions. This is summarized in Table 2 and is illustrated by Figure 9 showing the spectra of $|\delta|$ for each site and mission. On average, $|\delta|$ decreases from 0.03 at 443 nm to 0.015 in the NIR, with most curves within a factor of 2 (between 0.02 and 0.04 at 443 nm, and between 0.01 and 0.02 in the NIR). The results obtained for SeaWiFS show the highest level of dispersion between sites, which could be partly explained by the lower signal-to-noise ratio of this mission. For a given basin, the spectra of $|\delta|$ tend to be fairly close to each other, with some

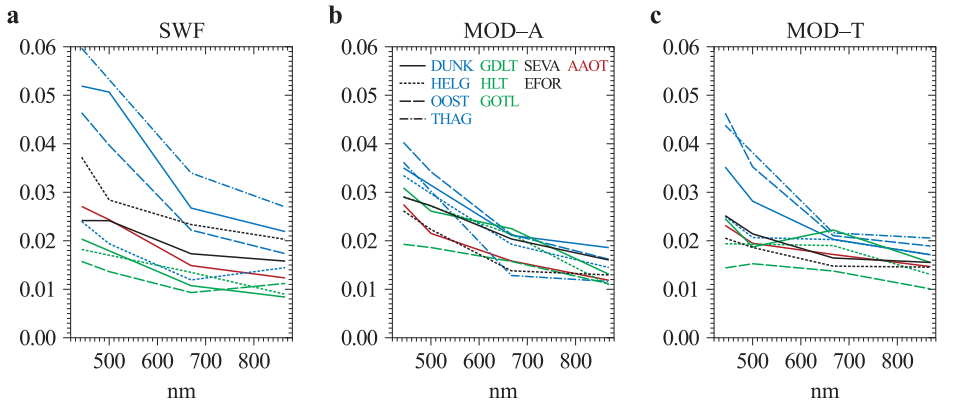

Figure 9. Comparison of median absolute differences $|\delta|$ for all sites for a) SeaWiFS, b) MODIS-A and c) MODIS-T. The blue, green, black and brown colours are for the North Sea, Baltic Sea, Black Sea and the AAOT sites respectively. The lines denote AAOT, SEVA, GDLT and DUNK, the dotted lines EFOR, HLT and HELG, the dashed lines GOTL and OOST, and the dotted-dashed lines THAG

exceptions. For instance, $|\delta|$ for SeaWiFS is significantly lower for the Helgoland site than for the three other North Sea sites, which show the highest $|\delta|$ values. Some of the differences between the sites can be explained by the different morphologies of the coastline around each site. In terms of bias, the statistics obtained for SeaWiFS are generally the most favourable, with slightly negative biases for all basins. In contrast, those obtained for both MODIS missions are almost all positive.

4.3. Additional elements of evaluation

For the sites considered, conditions typically associated with high aerosol loads such as desert dust or biomass burning smoke are rarely significant, with the exception of extreme events (e.g. Ansmann et al. 2003, Mattis et al. 2003, Derimian et al. 2012). However, it is still expected that continental and anthropogenic sources could create conditions of high τ_a that are excluded from the ocean colour processing by a conservative bright pixel detection criterion (for SeaWiFS, pixels are considered bright if the Rayleigh-corrected TOA reflectance at 865 nm > 0.027). So the τ_a distributions derived from ocean colour are truncated with respect to large τ_a and not necessarily representative of the full frequency distributions. The maximum values associated with the match-ups for the satellite τ_a in the NIR are from 0.21 (at 865 nm for SeaWiFS in the North Sea) to 0.28 (at 869 nm for both MODIS at AAOT). At 443 nm, the overall maximum is

0.66 (for MODIS-A at AAOT). To measure the impact of truncation on the distribution, an AERONET series of daily τ_a is constructed for each site, and general statistics are computed for the period with significant satellite coverage (see Figure 2; for the whole year at AAOT, for the period May–September for the Baltic Sea, March–October for the North Sea, and January–November for the Black Sea). The ratio of the average τ_a at 443 nm from valid satellite records to the average daily value from AERONET is usually < 1. It is lowest for AAOT and The Hague (approximately 0.78), and lies within the interval 0.79–0.91 for the sites at Dunkerque, Oostende and Gotland. It is slightly higher in the Black Sea (0.86–0.94 at Sevastopol, 0.89–0.96 at Eforie), while it is around 1 for Helgoland and the two Baltic offshore sites (GDLT and HLT). Obviously the impact of truncation on the general distribution of τ_a varies between sites but it is usually significant. The fact that the general statistics are less affected or not affected at all in the case of three offshore locations might suggest that the satellite τ_a distributions away from the coast (e.g. in the central Black, North and Baltic seas) are fairly representative of actual values.

Apart from this limitation, the validation results presented here are fairly satisfactory. Considering that most sites are located on land and that most pixels entering the validation protocol are close to the coast, they could even be regarded as conservative estimates of uncertainties, as discussed in Section 2.3. The accuracy objective of the MODIS atmosphere project is to derive τ_a within $\pm(0.03 + 0.05\tau_a)$ over the ocean (Remer et al. 2008). Validation studies have shown that the fraction of match-ups with a difference between MODIS and field measurements of $\tau_a < 0.03 + 0.05\tau_a$ (noted γ) varies between 57% and 66% for different wavelengths (from 550 to 870 nm, Remer et al. (2008), Bréon et al. (2011)). It is emphasized that the MODIS products just referred to are those associated with the aerosol component of the MODIS programme and are derived from specific bands and processing schemes. When computing the fraction of good retrievals γ for the three ocean colour missions, it appears that it is lowest for the North Sea sites, with 50–62% at 443 and 500 nm, and 68–78% for the red and NIR bands (Table 3). For the other three groups, $\gamma > 62\%$, 67%, 72% and 75% for 443 nm, 500 nm, the red and NIR bands respectively, and is often around 80% for red and NIR wavelengths. These results and other comparisons with other missions (e.g. Kahn et al. 2010) show that the aerosol products derived from the considered ocean colour missions have uncertainties at least as good as other products associated with dedicated aerosol processing chains.

Table 3. Validation statistics in the four regions for τ_a derived from SeaWiFS (SWF), MODIS-A and MODIS-T, expressed as γ (in %), the fraction of τ_a retrievals within $\pm(0.03 + 0.05\tau_a)$ of the field value

Region	AAOT			BLCK		
λ	SWF	MOD-A	MOD-T	SWF	MOD-A	MOD-T
443	66	65	72	64	66	70
500	67	74	76	68	68	72
RED	81	80	78	77	74	78
NIR	85	87	81	79	75	78
Region	BALT			NORS		
λ	SWF	MOD-A	MOD-T	SWF	MOD-A	MOD-T
443	81	62	70	50	55	55
500	87	75	73	56	58	62
RED	89	72	74	68	72	70
NIR	92	79	79	76	78	73

5. Conclusions

This validation exercise has focused on four European marginal seas for which fairly large uncertainties in ocean colour derived in-water products are reported. The distribution of the Ångström exponent found at the ten sites under consideration are comparable and suggest a strong influence of continental sources at all sites, even though local conditions and transport pathways eventually determine the actual aerosol composition.

The validation results are fairly satisfactory, with $|\psi|$ at 443 nm between 12% and 15% for the three missions at the AAOT and Black Sea sites, and from 13% to 26% at the Baltic and North Sea sites. The bias characterizing τ_a is usually slightly negative for SeaWiFS and positive for MODIS. The spectral shape of τ_a is well reproduced with the bias on the Ångström exponent varying between -0.216 and $+0.213$ in units of α (from -15% to $+14\%$), while the uncertainty $|\delta|$ is mostly < 0.3.

Most spectral curves of uncertainty $|\delta|$ associated with τ_a are found within a factor of 2, approximately between 0.02 and 0.04 at 443 nm, and between 0.01 and 0.02 in the NIR. It has been shown that high solar zenith angles, such as those found in the Baltic Sea, could affect the atmospheric correction (Bulgarelli et al. 2003), but the results obtained for sites at high latitudes do not display any systematic degradation. This relative consistency of the validation statistics observed for the three satellite missions is favoured by a common strategy for calibration (Franz et al. 2007) as well as a consistent processing chain. In this respect it is worth noting

that the MODIS mission on board Terra shows uncertainties comparable to the other two missions, even though the Terra products have been given less attention by the ocean colour community. This consistency is parallel to that observed for the validation of remote sensing reflectance in European waters (Zibordi et al. 2011, Mélin et al. 2011, 2012). These results are also very similar to those obtained from a global analysis (Mélin et al. 2013), even though the sites examined here present challenging conditions, with rather turbid coastal waters and complex aerosol mixtures. For comparison, $|\psi|$ at 443 nm associated with global statistics is 17%, 22% and 20% for SeaWiFS, MODIS-A and MODIS-T respectively. How this uncertainty regarding τ_a is translated into uncertainties with respect to R_{RS} depends on several factors, including the relationship between τ_a and the aerosol reflectance and the relative contribution of the aerosol reflectance to the TOA signal. Further improvements of the atmospheric correction in coastal waters may require an additional level of detail to describe the complex aerosol mixtures more accurately, and specific water bio-optical models for an appropriate representation of the boundary condition.

Acknowledgements

This work relies on the dedication of the scientists managing the AERONET systems at land stations or at sea, and we express our sincere gratitude for their contributions, in particular, that of the Principal Investigators for the sites of Dunkerque (P. Goloub and J.-F. Léon), Helgoland (R. Doerffer) and Oostende (K. Ruddick). We thank J.-P. De Blauwe thank for maintaining the Oostende site. The authors would also like to thank the Ocean Biology Processing Group of NASA for supplying us with the SeaWiFS and MODIS L1A data, and the European Space Agency, for direct provision of SeaWiFS imagery through three receiving stations for 2006–2007. This activity is also contributing to the Climate Change Initiative of the European Space Agency.

References

Ahmad Z., Franz B. A., McClain C. R., Kwiatkowska E. J., Werdell P. J., Shettle E. P., Holben B. N., 2010, *New aerosol models for the retrieval of aerosol optical thickness and normalized water-leaving radiances from the SeaWiFS and MODIS sensors over coastal regions and open oceans*, Appl. Opt., 49 (9), 5545–5560, http://dx.doi.org/10.1364/AO.49.005545.

Ansmann A., Bösenberg J., Chaikovsky A., Comerón A., Eckhardt S., Eixmann R., Freudenthaler V., Ginoux P., Komguem L., Linné H., López Márquez M. A., Matthias V., Mattis I., Mitev V., Müller D., Music S., Nickovic S.,

Pelon J., Sauvage L., Sobolewsky P., Srivastava M. K., Stohl A., Torres O., Vaughan G., Wandinger U., Wiegner M., 2003, *Long-range transport of Saharan dust to northern Europe: The 11–16 October 2001 outbreak observed with EARLINET*, J. Geophys. Res., 108 (D24), 4783, http://dx.doi.org/10.1029/2003JD003757.

Bailey S. W., Franz B. A., Werdell P. J., 2010, *Estimation of near-infrared water-leaving reflectance for satellite ocean color data processing*, Opt. Exp., 18 (7), 7521–7527, http://dx.doi.org/10.1364/OE.18.007521.

Bailey S. W., Werdell P. J., 2006, *A multi-sensor approach for the on-orbit validation of ocean color satellite data products*, Remote Sens. Environ., 102 (1–2), 12–23, http://dx.doi.org/10.1016/j.rse.2006.01.015.

Blondeau-Patissier D., Tilstone G.H., Martinez-Vicente V., Moore G. F., 2004, *Comparison of bio-physical marine products from SeaWiFS, MODIS and a bio-optical model with in situ measurements from Northern European waters*, J. Opt. A–Pure Appl. Op., 6 (9), 875–889, http://dx.doi.org/10.1088/1464-4258/6/9/010.

Bréon F.-M., Vermeulen A., Descloitres J., 2011, *An evaluation of satellite aerosol products against sunphotometer measurements*, Remote Sens. Environ., 115 (12), 3102–3111, http://dx.doi.org/10.1016/j.rse.2011.06.017.

Bulgarelli B., Mélin F., Zibordi G., 2003, *SeaWiFS-derived products in the Baltic Sea: performance analysis of a simple atmospheric correction algorithm*, Oceanologia, 45 (4), 655–677.

Carlund T., Håkansson B., Land P., 2005, *Aerosol optical depth over the Baltic Sea derived from AERONET and SeaWiFS measurements*, Int. J. Remote Sens., 26 (2), 233–245, http://dx.doi.org/10.1080/01431160410001720306.

Clerici M., Mélin F., 2008, *Aerosol direct radiative effect in the Po Valley region derived from AERONET measurements*, Atmos. Chem. Phys., 8 (16), 4925–4946, http://dx.doi.org/10.5194/acp-8-4925-2008.

Darecki M., Stramski D., 2004, *An evaluation of MODIS and SeaWiFS bio-optical algorithms in the Baltic Sea*, Remote Sens. Environ., 89 (3), 326–350, http://dx.doi.org/10.1016/j.rse.2003.10.012.

Derimian Y., Dubovik O., Tanré D., Goloub P., Lapyonok T., Mortier A., 2012, *Optical properties and radiative forcing of the Eyjafjallajökull volcanic ash layer observed over Lille, France, in 2010*, J. Geophys. Res., 117 (D9), D00U25, http://dx.doi.org/10.1029/2011JD016815.

Ebert M., Weinbruch S., Hoffmann P., Ortner H. M., 2000, *Chemical characterization of North Sea aerosol particles*, J. Aerosol Sci., 31 (5), 613–632, http://dx.doi.org/10.1016/S0021-8502(99)00549-2.

Eck T. F., Holben B. N., Reid J. S., Dubovik O., Smirnov A., O'Neill N. T., Slutsker I., Kinne S., 1999, *The wavelength dependence of the optical depth of biomass burning, urban and desert dust aerosols*, J. Geophys. Res., 104 (D24), 31333–31350, http://dx.doi.org/10.1029/1999JD900923.

Esaias W. E., Abbott M. R., Barton I., Brown O. B., Campbell J. W., Carder K. L., Clark D. K., Evans R. H., Hoge F. E., Gordon H. R., Balch W. M., Letelier R., Minnett P. J., 1998, *An overview of MODIS capabilities for ocean science observations*, IEEE Trans. Geosci. Remote Sens., 36 (4), 1250–1265, http://dx.doi.org/10.1109/36.701076.

Franz B. A., Bailey S. W., Werdell P. J., McClain C. R., 2007, *Sensor-independent approach to the vicarious calibration of satellite ocean color radiometry*, Appl. Opt., 46 (22), 5068–5082, http://dx.doi.org/10.1364/AO.46.005068.

Fu G., Baith K. S., McClain C. R., 1998, *SeaDAS: The SeaWiFS data analysis system*, Proc. 4th Pacific Ocean Remote Sens. Conf., Qingdao, China, July 28–31, 1998, 73–79.

Gordon H. R., Wang M., 1994, *Retrieval of water-leaving radiance and aerosol optical thickness over the oceans with SeaWiFS: a preliminary algorithm*, Appl. Opt., 33 (3), 443–452, http://dx.doi.org/10.1364/AO.33.000443.

Holben B. N., Eck T. F., Slutsker I., Tanré D., Buis J. P., Setzer A., Vermote E., Reagan J. A., Kaufman Y. J., Nakajima T., Lavenu F., Jankowiak I., Smirnov A., 1998, *AERONET – a federated instrument network and data archive for aerosol characterization*, Remote Sens. Environ., 66 (1), 1–16, http://dx.doi.org/10.1016/S0034-4257(98)00031-5.

Kahn R. A., Gaitley B. J., Garay M. J., Diner D. J., Eck T. F., Smirnov A., Holben B. N., 2010, *Multiangle Imaging SpectroRadiometer global aerosol product assessment by comparison with the Aerosol Robotic Network*, J. Geophys. Res., 115, D23209, http://dx.doi.org/10.1029/2010JD014601.

Koelemeijer R. B. A., Homan C. D., Matthijsen J., 2006, *Comparison of spatial and temporal variations of aerosol optical thickness and particulate matter over Europe*, Atmos. Environ., 40 (27), 5304–5315, http://dx.doi.org/10.1016/j.atmosenv.2006.04.044.

Kuśmierczyk-Michulec J., de Leeuw G., Moerman M. M., 2007, *Physical and optical aerosol at the Dutch North Sea coast based on AERONET observations*, Atmos. Chem. Phys., 7 (13), 3481–3495, http://dx.doi.org/10.5194/acp-7-3481-2007.

Lavender S. J., Pinkerton M. H., Froidefond J.-M., Morales J., Aiken J., Moore G. F., 2004, *SeaWiFS validation in European coastal waters using optical and bio-geochemical measurements*, Int. J. Remote Sens., 25 (7–8), 1481–1488, http://dx.doi.org/10.1080/01431160310001592481.

Marmer E., Langmann B., Fagerli H., Vestreng V., 2007, *Direct shortwave radiative forcing of sulfate aerosol over Europe from 1900 to 2000*, J. Geophys. Res., 112, D23S17, http://dx.doi.org/10.1029/2006JD008037.

Mattis I., Ansmann A., Wandinger U., Müller D., 2003, *Unexpectedly high aerosol load in the free troposphere over central Europe in spring/summer 2003*, Geophys. Res. Lett., 30 (22), 2178, http://dx.doi.org/10.1029/2003GL018442.

McArthur L. J. B., Halliwell D. H., Niebergall O. J., O'Neill N. T., Slusser J. R., Wehrli C., 2003, *Field comparison of network Sun photometers*, J. Geophys. Res., 108 (D19), 4596, http://dx.doi.org/10.1029/2002JD002964.

McClain C. R., Cleave M. L., Feldman G. C., Gregg W. W., Hooker S. B., Kuring N., 1998, *Science quality SeaWiFS data for global biosphere research*, Sea Tech., 39, 10–16.

Mélin F., Clerici M., Zibordi G., Bulgarelli B., 2006, *Aerosol variability in the Adriatic Sea from automated optical field measurements and SeaWiFS*, J. Geophys. Res., 111, D22201, http://dx.doi.org/10.1029/2006JD007226.

Mélin F., Clerici M., Zibordi G., Holben B. N., Smirnov A., 2010, *Validation of SeaWiFS and MODIS aerosol products with globally distributed AERONET data*, Remote Sens. Environ., 114 (2), 230–250, http://dx.doi.org/10.1016/j.rse.2009.09.003.

Mélin F., Zibordi G., 2005, *Aerosol variability in the Po Valley analyzed from automated optical measurements*, Geophys. Res. Lett., 32 (3), L03810, http://dx.doi.org/10.1029/2004GL021787.

Mélin F., Zibordi G., Berthon J.-F., 2007a, *Assessment of satellite ocean color products at a coastal site*, Remote Sens. Environ., 110 (2), 192–215, http://dx.doi.org/10.1016/j.rse.2007.02.026.

Mélin F., Zibordi G., Berthon J.-F., 2012, *Uncertainties in remote sensing reflectance from MODIS-Terra*, IEEE Geosci. Remote Sens. Lett., 9 (3), 432–436, http://dx.doi.org/10.1109/LGRS.2011.2170659.

Mélin F., Zibordi G., Berthon J.-F., Bailey S. W., Franz B. A., Voss K. J., Flora S., Grant M., 2011, *Assessment of MERIS reflectance data as processed with SeaDAS over the European seas*, Opt. Exp., 19 (25), 25657–25671, http://dx.doi.org/10.1364/OE.19.025657.

Mélin F., Zibordi G., Djavidnia S., 2007b, *Development and validation of a technique for merging satellite derived aerosol optical depth from SeaWiFS and MODIS*, Remote Sens. Environ., 108 (4), 436–450, http://dx.doi.org/10.1016/j.rse.2006.11.026.

Mélin F., Zibordi G., Holben B. N., 2013, *Assessment of the aerosol products from the SeaWiFS and MODIS ocean color missions*, IEEE Geosci. Remote Sens. Lett., (in press).

O'Neill N. T., Eck T. F., Holben B. N., Smirnov A., Dubovik O., Royer A., 2001, *Bimodal size distribution influences on the variation of Ångström derivatives in spectral and optical depth space*, J. Geophys. Res., 106 (D9), 9787–9806, http://dx.doi.org/10.1029/2000JD900245.

Remer L. A., Kleidman R. G., Levy R. C., Kaufman Y. J., Tanré D., Mattoo S., Martins J. V., Ichoku C., Koren I., Yu H., Holben B. N., 2008, *Global aerosol climatology from the MODIS satellite sensors*, J. Geophys. Res., 113, D14S07, 10.1029/2007JD009661.

Sancak S., Besiktepe S. T., Yilmaz A., Lee M., Frouin R., 2005, *Evaluation of SeaWiFS chlorophyll-a in the Black and Mediterranean Seas*, Int. J. Remote Sens., 26 (10), 2045–2060, http://dx.doi.org/10.1080/01431160512331337853.

Schmid B., Michalsky J., Halthore R., Beauharnois M., Harrison L., Livingston J., Russell P., Holben B. N., Eck T. F., Smirnov A., 1999, *Comparison of aerosol optical depth from four solar radiometers during the Fall 1997*

ARM intensive observation period, Geophys. Res. Lett., 26 (17), 2725–2728, http://dx.doi.org/10.1029/1999GL900513.

Sciare J., Oikonomou K., Favez O., Liakakou E., Markaki Z., Cachier H., Mihalopoulos N., 2008, *Long-term measurements of carbonaceous aerosols in the Eastern Mediterranean: evidence of long-range transport of biomass burning*, Atmos. Chem. Phys., 8 (14), 5551–5563, http://dx.doi.org/10.5194/acp-8-5551-2008.

Shettle E. P., Fenn R. W., 1979, *Models for the aerosols of the lower atmosphere and the effects of humidity variations on their optical properties*, Environ. Res. Paper, 676, AFGL-TR-79-0214 (U.S. Air Force Geophys. Lab., Hanscom A.F.B., MA), 1–94.

Smirnov A., Holben B. N., Eck T. F., Dubovik O., Slutsker I., 2000, *Cloud-screening and quality control algorithms for the AERONET database*, Remote Sens. Environ., 73 (3), 337–349, http://dx.doi.org/10.1016/S0034-4257(00)00109-7.

Smirnov A., Holben B. N., Lyapustin A., Slutsker I., Eck T. F., 2004, *AERONET processing algorithm refinement*, AERONET Workshop, El Arenosillo, Spain, May 10–14, 2004.

Toledano C., Cachorro V. E., Gausa M., Stebel K., Aaltonen V., Berjón A., Ortiz de Galisteo J. P., de Frutos A. M., Bennouna Y., Blindheim S., Myhre C. L., Zibordi G., Wehrli C., Kratzer S., Håkansson B., Carlund T., de Leeuw G., Herber A., Torres B., 2012, *Overview of sun photometer measurements of aerosol properties in Scandinavia and Svalbard*, Atmos. Environ., 52, 18–28, http://dx.doi.org/10.1016/j.atmosenv.2011.10.022.

Zdun A., Rozwadowska A., Kratzer S., 2011, *Seasonal variability in the optical properties of Baltic aerosols*, Oceanologia, 53 (1), 7–34, http://dx.doi.org/10.5697/oc.53-1.007.

Zibordi G., Berthon J.-F., Mélin F., D'Alimonte D., 2011, *Cross-site consistent in situ measurements for satellite ocean color applications: the BiOMaP radiometric dataset*, Remote Sens. Environ., 115 (8), 2104–2115, http://dx.doi.org/10.1016/j.rse.2011.04.013.

Zibordi G., Berthon J.-F., Mélin F., D'Alimonte D., Kaitala S., 2009, *Validation of satellite ocean color primary products at optically complex coastal sites: northern Adriatic Sea, northern Baltic Proper and Gulf of Finland*, Remote Sens. Environ., 113 (12), 2574–2591, http://dx.doi.org/10.1016/j.rse.2009.07.013.

Zibordi G., Mélin F., Berthon J.-F., 2012, *Trends in the bias of primary satellite ocean color products at a coastal site*, IEEE Geosci. Remote Sens. Lett., 9 (6), 1056–1060, http://dx.doi.org/10.1109/LGRS.2012.2189753.